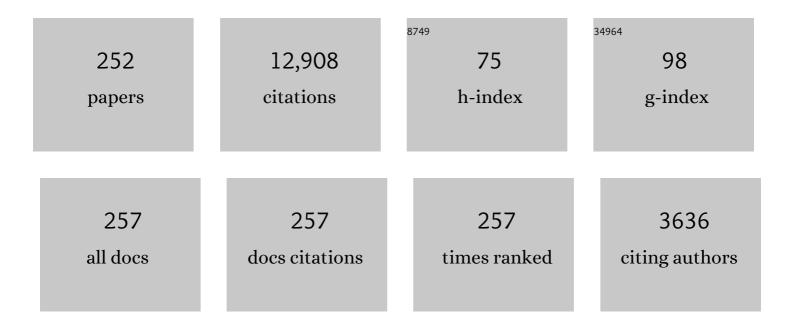
List of Publications by Year in descending order

Source: https://exaly.com/author-pdf/8823311/publications.pdf Version: 2024-02-01



#	Article	IF	CITATIONS
1	Crystal structure and magnetic properties of the BaFe12â^'Al O19 (x=0.1–1.2) solid solutions. Journal of Magnetism and Magnetic Materials, 2015, 393, 253-259.	1.0	287
2	Polarization origin and iron positions in indium doped barium hexaferrites. Ceramics International, 2018, 44, 290-300.	2.3	240
3	Control of electromagnetic properties in substituted M-type hexagonal ferrites. Journal of Alloys and Compounds, 2018, 754, 247-256.	2.8	214
4	Correlation Between Composition and Electrodynamics Properties in Nanocomposites Based on Hard/Soft Ferrimagnetics with Strong Exchange Coupling. Nanomaterials, 2019, 9, 202.	1.9	213
5	Ultrahigh enhancement rate of the energy density of flexible polymer nanocomposites using core–shell BaTiO ₃ @MgO structures as the filler. Journal of Materials Chemistry A, 2020, 8, 11124-11132.	5.2	178
6	Significantly enhanced electrostatic energy storage performance of P(VDF-HFP)/BaTiO3-Bi(Li0.5Nb0.5)O3 nanocomposites. Nano Energy, 2020, 78, 105247.	8.2	151
7	Magnetic state of the structural separated anion-deficient La0.70Sr0.30MnO2.85 manganite. Journal of Experimental and Theoretical Physics, 2011, 113, 819-825.	0.2	139
8	Investigation into the structural features and microwave absorption of doped barium hexaferrites. Dalton Transactions, 2017, 46, 9010-9021.	1.6	136
9	Preparation and investigation of structure, magnetic and dielectric properties of (BaFe11.9Al0.1O19)1 (BaTiO3) bicomponent ceramics. Ceramics International, 2018, 44, 21295-21302.	2.3	130
10	Crystal structure and magnetic properties of the BaFe12â^'In O19 (x=0.1–1.2) solid solutions. Journal of Magnetism and Magnetic Materials, 2016, 417, 130-136.	1.0	128
11	Fe3O4 Nanoparticles for Complex Targeted Delivery and Boron Neutron Capture Therapy. Nanomaterials, 2019, 9, 494.	1.9	128
12	Coexistence of spontaneous polarization and magnetization in substituted M-type hexaferrites BaFe12–x Al x O19 (x ⩽ 1.2) at room temperature. JETP Letters, 2016, 103, 100-105.	0.4	127
13	Impact of Eu3+ ion substitution on structural, magnetic and microwave traits of Ni–Cu–Zn spinel ferrites. Ceramics International, 2020, 46, 11124-11131.	2.3	126
14	Structure and magnetic properties of BaFe11.9In0.1O19 hexaferrite in a wide temperature range. Journal of Alloys and Compounds, 2016, 689, 383-393.	2.8	122
15	Magnetic properties and Mössbauer study of gallium doped M-type barium hexaferrites. Ceramics International, 2017, 43, 12822-12827.	2.3	121
16	Critical behavior of La0.825Sr0.175MnO2.912 anion-deficient manganite in the magnetic phase transition region. JETP Letters, 2007, 85, 507-512.	0.4	119
17	Magnetic anisotropy of the graphite nanoplatelet–epoxy and MWCNT–epoxy composites with aligned barium ferrite filler. Journal of Materials Science, 2017, 52, 5345-5358.	1.7	117
18	Immobilization of boron-rich compound on Fe3O4 nanoparticles: Stability and cytotoxicity. Journal of Alloys and Compounds, 2019, 797, 573-581.	2.8	117

#	Article	IF	CITATIONS
19	Magnetic and dipole moments in indium doped barium hexaferrites. Journal of Magnetism and Magnetic Materials, 2018, 457, 83-96.	1.0	113
20	Effect of the size factor on the magnetic properties of manganite La0.50Ba0.50MnO3. Physics of the Solid State, 2008, 50, 886-893.	0.2	111
21	Investigation of AC-Measurements of Epoxy/Ferrite Composites. Nanomaterials, 2020, 10, 492.	1.9	110
22	Multiferroic properties and structural features of M-type Al-substituted barium hexaferrites. Physics of the Solid State, 2017, 59, 737-745.	0.2	108
23	Frustrated exchange interactions formation at low temperatures and high hydrostatic pressures in La0.70Sr0.30MnO2.85. Journal of Experimental and Theoretical Physics, 2010, 111, 209-214.	0.2	107
24	Evolution of structure and magnetic properties for BaFe11.9Al0.1O19 hexaferrite in a wide temperature range. Journal of Magnetism and Magnetic Materials, 2017, 426, 487-496.	1.0	107
25	Correlation of the atomic structure, magnetic properties and microwave characteristics in substituted hexagonal ferrites. Journal of Magnetism and Magnetic Materials, 2018, 462, 127-135.	1.0	107
26	Electrophysical properties of epoxy-based composites with graphite nanoplatelets and magnetically aligned magnetite. Molecular Crystals and Liquid Crystals, 2018, 661, 68-80.	0.4	106
27	Magnetic, dielectric and microwave properties of the BaFe12-xGaxO19 (x ≤.2) solid solutions at room temperature. Journal of Magnetism and Magnetic Materials, 2017, 442, 300-310.	1.0	105
28	Electromagnetic properties of BaFe12O19:Ti at centimeter wavelengths. Journal of Alloys and Compounds, 2018, 755, 177-183.	2.8	105
29	Influence of the charge ordering and quantum effects in heterovalent substituted hexaferrites on their microwave characteristics. Journal of Alloys and Compounds, 2019, 788, 1193-1202.	2.8	105
30	Thermal evolution of exchange interactions in lightly doped barium hexaferrites. Journal of Magnetism and Magnetic Materials, 2017, 426, 554-562.	1.0	104
31	Synthesis of barium ferrite nanoparticles using rhizome extract of Acorus Calamus: Characterization and its efficacy against different plant phytopathogenic fungi. Nano Structures Nano Objects, 2020, 24, 100599.	1.9	104
32	Strong correlation between Dy3+ concentration, structure, magnetic and microwave properties of the [Ni0.5Co0.5](DyxFe2-x)O4 nanosized ferrites. Journal of Industrial and Engineering Chemistry, 2020, 90, 251-259.	2.9	103
33	Critical influence of different diamagnetic ions on electromagnetic properties of BaFe12O19. Ceramics International, 2018, 44, 13520-13529.	2.3	102
34	Magnetic and microwave properties of SrFe12O19/MCe0.04Fe1.96O4 (M = Cu, Ni, Mn, Co and Zn) hard/soft nanocomposites. Journal of Materials Research and Technology, 2020, 9, 5858-5870.	2.6	102
35	Magnetic properties of anion deficit manganites Ln0.55Ba0.45MnO3â^î³ (Ln=La, Nd, Sm, Gd, γ⩼20.37). Journa of Magnetism and Magnetic Materials, 2000, 208, 217-220.	al 1.0	101
36	Ni substitution effect on the structure, magnetization, resistivity and permeability of zinc ferrites. Journal of Materials Chemistry C, 2021, 9, 5425-5436.	2.7	101

#	Article	IF	CITATIONS
37	Pecularities of the magnetic structure and microwave properties in Ba(Fe1-xScx)12O19 (x<0.1) hexaferrites. Journal of Alloys and Compounds, 2020, 822, 153575.	2.8	100
38	Effect of gallium doping on electromagnetic properties of barium hexaferrite. Journal of Physics and Chemistry of Solids, 2017, 111, 142-152.	1.9	99
39	Investigation of structural and physical properties of Eu3+ ions substituted Ni0.4Cu0.2Zn0.4Fe2O4 spinel ferrite nanoparticles prepared via sonochemical approach. Results in Physics, 2020, 17, 103061.	2.0	99
40	Temperature evolution of the structure parameters and exchange interactions in BaFe12â^'xlnxO19. Journal of Magnetism and Magnetic Materials, 2018, 466, 393-405.	1.0	98
41	Crystal and magnetic structures, magnetic and ferroelectric properties of strontium ferrite partially substituted with in ions. Journal of Alloys and Compounds, 2020, 821, 153412.	2.8	98
42	Strong corelation between magnetic and electrical subsystems in diamagnetically substituted hexaferrites ceramics. Ceramics International, 2017, 43, 5635-5641.	2.3	97
43	Control of Growth Mechanism of Electrodeposited Nanocrystalline NiFe Films. Journal of the Electrochemical Society, 2019, 166, D173-D180.	1.3	97
44	Evolution of magnetic state in the La1â^'xCaxMnO3â^'î³ (x=0.30, 0.50) manganites depending on the oxygen content. Journal of Solid State Chemistry, 2002, 169, 85-95.	1.4	96
45	Magnetotransport Properties and Mechanism of the A-Site Ordering in the Nd–Ba Optimal-Doped Manganites. Journal of Low Temperature Physics, 2007, 149, 185-199.	0.6	95
46	Magnetic and absorbing properties of M-type substituted hexaferrites BaFe12–x Ga x O19 (0.1 < x <) Tj ET	2g0 0 0 r _{	gBT /Overloc
47	xmlns:mml="http://www.w3.org/1998/Math/MathML" altimg="si1.gif" overflow="scroll"> <mml:mrow><mml:mrow><mml:mi mathvariant="italic">BaFe</mml:mi </mml:mrow><mml:mrow><mml:mn>12</mml:mn><mml:mo>-</mml:mo>< mathvariant="italic">Me</mml:mrow><mml:mrow><mml:mi>x</mml:mi></mml:mrow>xx</mml:mrow> xxxxxxxxxxxxxx <td>1.0 mml:mi>> mml:msu</td> <td>< ∕< b> < mml:mro</td>	1.0 mml:mi>> mml:msu	< ∕< b> < mml:mro
48	Journal of Magnetism and Magnetic Materials, 2018, 464, 139-147. Magnetic Attributes of NiFe2O4 Nanoparticles: Influence of Dysprosium Ions (Dy3+) Substitution. Nanomaterials, 2019, 9, 820.	1.9	95
49	Effect of magnetic fillers and their orientation on the electrodynamic properties of BaFe12-xGaxO19 (x = 0.1–1.2)—epoxy composites with carbon nanotubes within GHz range. Applied Nanoscience (Switzerland), 2020, 10, 4747-4752.	1.6	95
50	Thermal stability of A-site ordered PrBaMn2O6 manganites. Journal of Physics and Chemistry of Solids, 2006, 67, 675-681.	1.9	94
51	Correlation of crystalline and magnetic structures of barium ferrites with dual ferroic properties. Journal of Magnetism and Magnetic Materials, 2019, 477, 9-16.	1.0	94
52	Anomalies in Ni-Fe nanogranular films growth. Journal of Alloys and Compounds, 2018, 748, 970-978.	2.8	93
53	Features of crystal and magnetÑ–c structure of the BaFe12-xGaxO19 (x â‰ 8 €¯2) in the wÑ–de temperature ra Journal of Alloys and Compounds, 2019, 791, 522-529.	ange. 2.8	93
54	Peculiarities of the microwave properties of hard–soft functional composites SrTb _{0.01} Tm _{0.01} Fe _{11.98} O ₁₉ –AFe ₂ O (A = Co, Ni, Zn, Cu, or Mn). RSC Advances, 2020, 10, 32638-32651.	<b £.	92

#	Article	IF	CITATIONS
55	Specifics of pyrohydrolytic and solid-phase syntheses of solid solutions in the (MgGa2O4) x (MgFe2O4)1 â^' x system. Russian Journal of Inorganic Chemistry, 2010, 55, 427-429.	0.3	91
56	Effect of magnetic fields on magnetic phase separation in anion-deficient manganite La0.70Sr0.30MnO2.85. Low Temperature Physics, 2011, 37, 465-469.	0.2	91
57	Features of the Growth Processes and Magnetic Domain Structure of NiFe Nano-objects. Journal of Physical Chemistry C, 2019, 123, 26957-26964.	1.5	91
58	Effectiveness of the magnetostatic shielding by the cylindrical shells. Journal of Magnetism and Magnetic Materials, 2016, 398, 49-53.	1.0	90
59	Functional Magnetic Composites Based on Hexaferrites: Correlation of the Composition, Magnetic and High-Frequency Properties. Nanomaterials, 2019, 9, 1720.	1.9	90
60	Investigation of the crystal and magnetic structures of BaFe12 - x Al x O19 solid solutions (x = 0.1‒1.2). Crystallography Reports, 2015, 60, 629-635.	0.1	89
61	Evolution of structure and physical properties in Al-substituted Ba-hexaferrites. Chinese Physics B, 2016, 25, 016102.	0.7	89
62	Magnetic properties of La0.70Sr0.30MnO2.85 anion-deficient manganite under hydrostatic pressure. JETP Letters, 2006, 83, 33-36.	0.4	88
63	Electrochemical deposition regimes and critical influence of organic additives on the structure of Bi films. Journal of Alloys and Compounds, 2018, 735, 1943-1948.	2.8	87
64	Study of the crystalline and magnetic structures of BaFe11.4Al0.6O19 in a wide temperature range. Journal of Surface Investigation, 2015, 9, 17-23.	0.1	86
65	AC and DC-shielding properties for the Ni80Fe20/Cu film structures. Journal of Magnetism and Magnetic Materials, 2017, 443, 142-148.	1.0	86
66	Crystal structure and magnetic properties of Ba-ordered manganites Ln0.70Ba0.30MnO3â~'δ (Ln = Pr, Nd). Journal of Experimental and Theoretical Physics, 2006, 103, 398-410.	0.2	84
67	Influence of Nd-NbZn co-substitution on structural, spectral and magnetic properties of M-type calcium-strontium hexaferrites Ca0.4Sr0.6-xNdxFe12.0-x(Nb0.5Zn0.5)xO19. Journal of Alloys and Compounds, 2018, 765, 616-623.	2.8	84
68	The effect of Nb substitution on magnetic properties of BaFe12O19 nanohexaferrites. Ceramics International, 2019, 45, 1691-1697.	2.3	84
69	Study of A-site ordered PrBaMn2O6â^îŕmanganite properties depending on the treatment conditions. Journal of Physics Condensed Matter, 2005, 17, 6495-6506.	0.7	81
70	High hydrostatic pressure effect on magnetic state of anion-deficient La0.70Sr0.30MnOx perovskite manganites. Journal of Magnetism and Magnetic Materials, 2008, 320, e88-e91.	1.0	81
71	Tuning the Structure, Magnetic, and High Frequency Properties of Scâ€Doped Sr _{0.5} Ba _{0.5} Sc <i>_x</i> Fe _{12â€} <i>_x</i> O _{ Hard/Soft Nanocomposites. Advanced Electronic Materials, 2022, 8, .}	19<2s6b>/	NiF ø ₄sub>2≪
72	Effect of treatment conditions on structure and magnetodielectric properties of barium hexaferrites. Journal of Magnetism and Magnetic Materials, 2020, 498, 166190.	1.0	80

#	Article	IF	CITATIONS
73	Synthesis and structure of nanocrystalline La0.50Ba0.50MnO3. Crystallography Reports, 2008, 53, 1177-1180.	0.1	79
74	Manganese/Yttrium Codoped Strontium Nanohexaferrites: Evaluation of Magnetic Susceptibility and Mossbauer Spectra. Nanomaterials, 2019, 9, 24.	1.9	77
75	Features of structure, magnetic state and electrodynamic performance of SrFe12â^'xlnxO19. Scientific Reports, 2021, 11, 18342.	1.6	77
76	Structural parameters, energy states and magnetic properties of the novel Se-doped NiFe2O4 ferrites as highly efficient electrocatalysts for HER. Ceramics International, 2022, 48, 24866-24876.	2.3	77
77	Impact of the Nanocarbon on Magnetic and Electrodynamic Properties of the Ferrite/Polymer Composites. Nanomaterials, 2022, 12, 868.	1.9	73
78	Correlation of the synthesis conditions and microstructure for Bi-based electron shields production. Journal of Alloys and Compounds, 2018, 749, 1036-1042.	2.8	72
79	Measurement of permittivity and permeability of barium hexaferrite. Journal of Magnetism and Magnetic Materials, 2018, 465, 290-294.	1.0	72
80	The Effect of Heat Treatment on the Microstructure and Mechanical Properties of 2D Nanostructured Au/NiFe System. Nanomaterials, 2020, 10, 1077.	1.9	72
81	Functional Sr0.5Ba0.5Sm0.02Fe11.98O4/x(Ni0.8Zn0.2Fe2O4) Hard–Soft Ferrite Nanocomposites: Structure, Magnetic and Microwave Properties. Nanomaterials, 2020, 10, 2134.	1.9	71
82	Phase separation and size effects in Pr0.70Ba0.30MnO3+δperovskite manganites. Journal of Physics Condensed Matter, 2007, 19, 266214.	0.7	70
83	Effect of the Synthesis Conditions and Microstructure for Highly Effective Electron Shields Production Based on Bi Coatings. ACS Applied Energy Materials, 2018, 1, 1695-1702.	2.5	65
84	Effect of Ga content on magnetic properties of BaFe12â^'xGaxO19/epoxy composites. Journal of Materials Science, 2020, 55, 9385-9395.	1.7	65
85	Impact of the heat treatment conditions on crystal structure, morphology and magnetic properties evolution in BaM nanohexaferrites. Journal of Alloys and Compounds, 2021, 866, 158961.	2.8	65
86	Ultra-low temperature co-fired ceramics with adjustable microwave dielectric properties in the Na ₂ O–Bi ₂ O ₃ –MoO ₃ ternary system: a comprehensive study. Journal of Materials Chemistry C, 2022, 10, 2008-2016.	2.7	65
87	An ultra-broadband terahertz metamaterial coherent absorber using multilayer electric ring resonator structures based on anti-reflection coating. Nanoscale, 2020, 12, 9769-9775.	2.8	64
88	Structure and magnetodielectric properties of titanium substituted barium hexaferrites. Ceramics International, 2021, 47, 17293-17306.	2.3	64
89	Electromagnetic Properties of Carbon Nanotube/BaFe12â°'xGaxO19/Epoxy Composites with Random and Oriented Filler Distributions. Nanomaterials, 2021, 11, 2873.	1.9	64
90	Function composites materials for shielding applications: Correlation between phase separation and attenuation properties. Journal of Alloys and Compounds, 2019, 771, 238-245.	2.8	63

#	Article	IF	CITATIONS
91	Review on functional bi-component nanocomposites based on hard/soft ferrites: Structural, magnetic, electrical and microwave absorption properties. Nano Structures Nano Objects, 2021, 26, 100728.	1.9	63
92	Peculiarities of the Crystal Structure Evolution of BiFeO3–BaTiO3 Ceramics across Structural Phase Transitions. Nanomaterials, 2020, 10, 801.	1.9	62
93	Effect of Co content on magnetic features and SPIN states IN Ni–Zn spinel ferrites. Ceramics International, 2021, 47, 12163-12169.	2.3	62
94	Structural and Magnetic Properties of Co0.5Ni0.5Ga0.01Gd0.01Fe1.98O4/ZnFe2O4 Spinel Ferrite Nanocomposites: Comparative Study between Sol-Gel and Pulsed Laser Ablation in Liquid Approaches. Nanomaterials, 2021, 11, 2461.	1.9	62
95	Effect of titanium substitution and temperature variation on structure and magnetic state of barium hexaferrites. Journal of Alloys and Compounds, 2021, 859, 158365.	2.8	61
96	Method of surface energy investigation by lateral AFM: application to control growth mechanism of nanostructured NiFe films. Scientific Reports, 2020, 10, 14411.	1.6	60
97	Study of comprehensive shielding behaviors of chambersite deposit for neutron and gamma ray. Progress in Nuclear Energy, 2022, 146, 104155.	1.3	60
98	Experimental and Theoretical Study of Radiation Shielding Features of CaO-K2O-Na2O-P2O5 Class Systems. Materials, 2021, 14, 3772.	1.3	59
99	Electrochemical Behaviour of Ti/Al2O3/Ni Nanocomposite Material in Artificial Physiological Solution: Prospects for Biomedical Application. Nanomaterials, 2020, 10, 173.	1.9	55
100	Influence of titanium substitution on structure, magnetic and electric properties of barium hexaferrites BaFe12â^'xTixO19. Journal of Magnetism and Magnetic Materials, 2020, 498, 166117.	1.0	53
101	Early-Stage Growth Mechanism and Synthesis Conditions-Dependent Morphology of Nanocrystalline Bi Films Electrodeposited from Perchlorate Electrolyte. Nanomaterials, 2020, 10, 1245.	1.9	53
102	Correlation between entropy state, crystal structure, magnetic and electrical properties in M-type Ba-hexaferrites. Journal of the European Ceramic Society, 2020, 40, 4022-4028.	2.8	52
103	Structural features, magnetic and ferroelectric properties of SrFe10.8In1.2O19 compound. Materials Research Bulletin, 2021, 138, 111236.	2.7	52
104	Changes in the Structure, Magnetization, and Resistivity of BaFe _{12–<i>x</i>} Ti <i>_x</i> O ₁₉ . ACS Applied Electronic Materials, 2021, 3, 1583-1593.	2.0	51
105	Electrocatalytic activity of various hexagonal ferrites in OER process. Materials Chemistry and Physics, 2021, 270, 124818.	2.0	51
106	lsostatic Hot Pressed W–Cu Composites with Nanosized Grain Boundaries: Microstructure, Structure and Radiation Shielding Efficiency against Gamma Rays. Nanomaterials, 2022, 12, 1642.	1.9	51
107	Developing the magnetic, dielectric and anticandidal characteristics of SrFe12O19/(Mg0.5Cd0.5Dy0.03Fe1.97O4)x hard/soft ferrite nanocomposites. Journal of the Taiwan Institute of Chemical Engineers, 2020, 113, 344-362.	2.7	50
108	Modeling of paths and energy losses of high-energy ions in single-layered and multilayered materials. IOP Conference Series: Materials Science and Engineering, 2020, 848, 012089.	0.3	49

#	Article	IF	CITATIONS
109	Upcycling of boron bearing blast furnace slag as highly cost-effective shield for protection of neutron radiation hazard: An innovative way and proposal of shielding mechanism. Journal of Cleaner Production, 2022, 355, 131817.	4.6	49
110	Fully Active Bimetallic Phosphide Zn _{0.5} Ge _{0.5} P: A Novel High-Performance Anode for Na-Ion Batteries Coupled with Diglyme-Based Electrolyte. ACS Applied Materials & Interfaces, 2022, 14, 31803-31813.	4.0	48
111	Fabrication of exchange coupled hard/soft magnetic nanocomposites: Correlation between composition, magnetic, optical and microwave properties. Arabian Journal of Chemistry, 2021, 14, 102992.	2.3	46
112	Flowery In2MnSe4 Novel Electrocatalyst Developed via Anion Exchange Strategy for Efficient Water Splitting. Nanomaterials, 2022, 12, 2209.	1.9	46
113	Magnetic and electrical properties of (Feln2S4)1â^'(Culn5S8) solid solutions. Journal of Magnetism and Magnetic Materials, 2015, 379, 22-27.	1.0	45
114	Influence of Dy ³⁺ Ions on the Microstructures and Magnetic, Electrical, and Microwave Properties of [Ni _{0.4} Cu _{0.2} Zn _{0.4}](Fe _{2–<i>x</i>} Dy _{<i>x</i>}) (0.00 ≤i>x ≤0.04) Spinel Ferrites. ACS Omega, 2021, 6, 10266-10280.	⊃{\$ub>4<	/sub>
115	Formation and corrosion properties of Ni-based composite material in the anodic alumina porous matrix. Journal of Alloys and Compounds, 2019, 804, 139-146.	2.8	44
116	Control of structural parameters and thermal conductivity of BeO ceramics using heavy ion irradiation and post-radiation annealing. Ceramics International, 2019, 45, 15412-15416.	2.3	43
117	Thermal Stability of Nano-Crystalline Nickel Electrodeposited into Porous Alumina. Solid State Phenomena, 0, 299, 281-286.	0.3	43
118	Electromagnetic properties of zinc–nickel ferrites in the frequency range of 0.05–10ÂGHz. Materials Today Chemistry, 2021, 20, 100460.	1.7	43
119	Combined Effect of Microstructure, Surface Energy, and Adhesion Force on the Friction of PVA/Ferrite Spinel Nanocomposites. Nanomaterials, 2022, 12, 1998.	1.9	43
120	Preparation and morphology-dependent wettability of porous alumina membranes. Beilstein Journal of Nanotechnology, 2018, 9, 1423-1436.	1.5	42
121	Impact of Tm3+ and Tb3+ Rare Earth Cations Substitution on the Structure and Magnetic Parameters of Co-Ni Nanospinel Ferrite. Nanomaterials, 2020, 10, 2384.	1.9	42
122	Cation ordering and magnetic properties of neodymium-barium manganites. Technical Physics, 2008, 53, 49-54.	0.2	41
123	Influence of Tm–Tb substitution on magnetic and optical properties of Ba–Sr hexaferrites prepared by ultrasonic assisted citrate sol-gel approach. Materials Chemistry and Physics, 2020, 253, 123324.	2.0	41
124	The influence of the synthesis conditions on the magnetic behaviour of the densely packed arrays of Ni nanowires in porous anodic alumina membranes. RSC Advances, 2021, 11, 3952-3962.	1.7	40
125	Impact of Sm ³⁺ and Er ³⁺ Cations on the Structural, Optical, and Magnetic Traits of Spinel Cobalt Ferrite Nanoparticles: Comparison Investigation. ACS Omega, 2022, 7, 6292-6301.	1.6	40
126	Structure, Morphology and Electrical/Magnetic Properties of Ni-Mg Nano-Ferrites from a New Perspective. Nanomaterials, 2022, 12, 1045.	1.9	40

#	Article	IF	CITATIONS
127	Synthesis, phase composition and structural and conductive properties of ferroelectric microparticles based on ATiOx (A = Ba, Ca, Sr). Ceramics International, 2019, 45, 17236-17242.	2.3	39
128	High-frequency absorption properties of gallium weakly doped barium hexaferrites. Philosophical Magazine, 2019, 99, 585-605.	0.7	39
129	The origin of the dual ferroic properties in quasi-centrosymmetrical SrFe12â^'xInxO19 hexaferrites. Journal of Alloys and Compounds, 2021, 886, 161249.	2.8	37
130	Investigation of exchange coupling and microwave properties of hard/soft (SrNi0.02Zr0.01Fe11.96O19)/(CoFe2O4)x nanocomposites. Materials Today Nano, 2022, 18, 100186.	2.3	37
131	Structural, Magnetic, and AC Measurements of Nanoferrites/Graphene Composites. Nanomaterials, 2022, 12, 931.	1.9	37
132	Properties of Mg(Fe1 â^' x Ga x)2O4 + δ solid solutions in stable and metastable states. Inorganic Materials, 2010, 46, 429-433.	0.2	35
133	Electronic, magnetic, and microwave properties of hard/soft nanocomposites based on hexaferrite SrNi0.02Zr0.02Fe11.96O19 with variable spinel phase MFe2O4 (M = Mn, Co, Cu, and Zn). Ceramics International, 2021, 47, 35209-35223.	2.3	35
134	Correlation between chemical composition, electrical, magnetic and microwave properties in Dy-substituted Ni-Cu-Zn ferrites. Materials Science and Engineering B: Solid-State Materials for Advanced Technology, 2021, 270, 115202.	1.7	34
135	Effect of Nd-Y co-substitution on structural, magnetic, optical and microwave properties of NiCuZn nanospinel ferrites. Journal of Materials Research and Technology, 2020, 9, 11278-11290.	2.6	33
136	Fabrication of hierarchical MoO3@NixCo2x(OH)6x core–shell arrays on carbon cloth as enhanced-performance electrodes for asymmetric supercapacitors. Journal of Colloid and Interface Science, 2022, 607, 1253-1261.	5.0	32
137	Heterovalent substituted BaFe12-xSnxO19 (0.1≤ ≤.2) M-type hexaferrite: Chemical composition, phase separation, magnetic properties and electrodynamics features. Journal of Alloys and Compounds, 2022, 896, 163117.	2.8	32
138	Development of tungsten doped Ni-Zn nano-ferrites with fast response and recovery time for hydrogen gas sensing application. Results in Physics, 2019, 15, 102531.	2.0	31
139	A New Approach to the Formation of Nanosized Gold and Beryllium Films by Ion-Beam Sputtering Deposition. Nanomaterials, 2022, 12, 470.	1.9	30
140	Anomalous dielectric behaviour during the monoclinic to tetragonal phase transition in La(Nb _{0.9} V _{0.1})O ₄ . Inorganic Chemistry Frontiers, 2021, 8, 156-163.	3.0	29
141	Electrical and dielectric properties of rare earth substituted hard-soft ferrite (Co0.5Ni0.5Ga0.01Gd0.01Fe1.98O4)x/(ZnFe2O4)y nanocomposites. Journal of Materials Research and Technology, 2021, 15, 969-983.	2.6	28
142	Experimental and theoretical analysis of radiation shielding properties of strontium-borate-tellurite glasses. Optical Materials, 2021, 121, 111589.	1.7	28
143	Electrodeposition conditions-dependent crystal structure, morphology and electronic properties of Bi films. Journal of Alloys and Compounds, 2021, 887, 161451.	2.8	28
144	Influence of cobalt substitution on structural, optical, electrical and magnetic properties of nanosized lithium ferrite. Journal of Materials Science: Materials in Electronics, 2018, 29, 16507-16515.	1.1	27

ALEX V TRUKHANOV

#	Article	IF	CITATIONS
145	The Conductivity and Dielectric Properties of Neobium Substituted Sr-Hexaferrites. Nanomaterials, 2019, 9, 1168.	1.9	27
146	A correlation between crystal structure and magnetic properties in co-doped BiFeO3 ceramics. Journal of Physics and Chemistry of Solids, 2019, 126, 164-169.	1.9	27
147	Ferrimagnetic-Paramagnetic Phase Transition in BaFe11.7In0.3O19 Compound. Journal of Superconductivity and Novel Magnetism, 2020, 33, 2867-2873.	0.8	26
148	Magnetic Properties of the Densely Packed Ultra-Long Ni Nanowires Encapsulated in Alumina Membrane. Nanomaterials, 2021, 11, 1775.	1.9	26
149	Temperature-Induced structural phase transformations in Cu1.50Zn0.30Te and Cu1.75Cd0.05Te single crystals. Crystallography Reports, 2017, 62, 610-617.	0.1	25
150	Effect of Fe doping on structure, magnetic and electrical properties La0.7Ca0.3Mn0.5Fe0.5O3 manganite. Ceramics International, 2018, 44, 14974-14979.	2.3	25
151	Microstructure, dielectric and microwave features of [Ni0.4Cu0.2Zn0.4](Fe2â^'Tb)O4 (x≤0.1) nanospinel ferrites. Journal of Materials Research and Technology, 2020, 9, 10608-10623.	2.6	25
152	Features of crystal and magnetic structures of solid solutions BaFe12-xDxO19 (D=Al3+, In3+; x=0.1) in a wide temperature range. European Physical Journal Plus, 2016, 131, 1.	1.2	24
153	Structural and magnetic transformations in amorphous ferromagnetic microwires during thermomagnetic treatment under conditions of directional crystallization. Journal of Alloys and Compounds, 2017, 698, 685-691.	2.8	24
154	Magnetic and microwave properties of carbonyl iron in the high frequency range. Journal of Magnetism and Magnetic Materials, 2019, 490, 165493.	1.0	24
155	Polysubstituted High-Entropy [LaNd](Cr0.2Mn0.2Fe0.2Co0.2Ni0.2)O3 Perovskites: Correlation of the Electrical and Magnetic Properties. Nanomaterials, 2021, 11, 1014.	1.9	24
156	Crystal structure, magnetic properties, and raman spectra of solid solutions BaFe12–x Al x O19. Physics of the Solid State, 2016, 58, 992-996.	0.2	23
157	Structure and piezoelectric properties of Sm-doped BiFeO3 ceramics near the morphotropic phase boundary. Materials Research Bulletin, 2019, 112, 420-425.	2.7	22
158	Interface magnetoelectric effect in elastically linked Co/PZT/Co layered structures. Journal of Magnetism and Magnetic Materials, 2019, 485, 291-296.	1.0	22
159	Extremely Polysubstituted Magnetic Material Based on Magnetoplumbite with a Hexagonal Structure: Synthesis, Structure, Properties, Prospects. Nanomaterials, 2019, 9, 559.	1.9	22
160	Can hexaferrite composites be used as a new artificial material for antenna applications?. Ceramics International, 2021, 47, 2615-2623.	2.3	22
161	Temperature-Stable <i>x</i> (Na _{0.5} Bi _{0.5})MoO ₄ –(1– <i>x</i>)MoO ₃ Composite Ceramics with Ultralow Sintering Temperatures and Low Dielectric Loss for Dielectric Resonator Antenna Applications, ACS Applied Electronic Materials, 2021, 3, 2286-2296.	2.0	22
162	Graphene Oxide Nanoparticles Modified Paper Electrode as a Biosensing Platform for Detection of the htrA Gene of O. tsutsugamushi. Sensors, 2021, 21, 4366.	2.1	22

#	Article	IF	CITATIONS
163	Crystal structure, magnetic, and microwave properties of solid solutions BaFe12–x Ga x O19 (0.1 ≤ â‰⊅Tj l	ETQq1 1 (0.2	0. <u>78</u> 4314 g
164	Flux single crystal growth of M-type strontium hexaferrite SrFe12O19 by spontaneous crystallization. Journal of Magnetism and Magnetic Materials, 2019, 470, 97-100.	1.0	20
165	Impact of the A-site rare-earth ions (Ln3+ – Sm3+, Eu3+, Gd3+) on structure and electrical properties of the high entropy LnCr0.2Mn0.2Fe0.2Co0.2Ni0.2O3 perovskites. Ceramics International, 2022, 48, 9239-9247.	2.3	20
166	Tb3+ ion substituted Sr-hexaferrites as high quality microwave absorbers. Journal of Magnetism and Magnetic Materials, 2019, 491, 165595.	1.0	19
167	Impact of the exfoliated graphite on magnetic and microwave properties of the hexaferrite-based composites. Journal of Alloys and Compounds, 2021, 878, 160397.	2.8	19
168	Investigation on electrical and dielectric properties of hard/soft spinel ferrite nanocomposites of CoFe2O4/(NiSc0.03Fe1.97O4)x. Vacuum, 2021, 194, 110628.	1.6	19
169	Specific features of formation and growth mechanism of multilayered quasi-one-dimensional (Co-Ni-Fe)/Cu systems in pores of anodic alumina matrices. Crystallography Reports, 2014, 59, 744-748.	0.1	18
170	Morphology and magnetic properties of pressed barium hexaferrite BaFe12O19 materials. Journal of Magnetism and Magnetic Materials, 2018, 459, 131-135.	1.0	18
171	Impact of the Zr-substitution on phase composition, structure, magnetic, and microwave properties of the BaM hexaferrite. Ceramics International, 2021, 47, 16752-16761.	2.3	18
172	Creation and Magnetic Study of Ferrites with Magnetoplumbite Structure Multisubstituted by Al3+, Cr3+, Ga3+, and In3+ Cations. Nanomaterials, 2022, 12, 1306.	1.9	18
173	Magnetotransport properties and calculation of the stability of GMR coefficients in CoNi/Cu multilayer quasi-one-dimensional structures. Materials Research Express, 2016, 3, 065010.	0.8	17
174	Influence of cation substitution on the polymorphic transformation in Ag2â€"Ñ Cu Ñ S (Ñ = 0.45, 0.8, and) T	j ETQq0 () Q _. rgBT /Ov
175	A Study of Ta2O5 Nanopillars with Ni Tips Prepared by Porous Anodic Alumina Through-Mask Anodization. Nanomaterials, 2022, 12, 1344.	1.9	17
176	Concentration-dependent structural transition in the La0.70Sr0.30MnO3â^îſ´system. JETP Letters, 2006, 84, 254-257.	0.4	16
177	Preparation and investigation of the magnetoelectric properties in layered cermet structures. Ceramics International, 2019, 45, 13030-13036.	2.3	16
178	Active control scattering manipulation for realization of switchable EIT-like response metamaterial. Optics Communications, 2021, 483, 126664.	1.0	16
179	Structure, Mössbauer and AC susceptibility of strontium nanohexaferrites: Effect of vanadium ions doping. Ceramics International, 2019, 45, 11615-11624.	2.3	15
180	Facile synthesis of calcium magnesium zirconium phosphate adsorbents transformed into MZr4P6O24 (M: Ca, Mg) ceramic matrix for radionuclides immobilization. Separation and Purification Technology, 2021, 272, 118912.	3.9	15

ALEX V TRUKHANOV

#	Article	IF	CITATIONS
181	A-Site Cation Size Effect on Structure and Magnetic Properties of Sm(Eu,Gd)Cr0.2Mn0.2Fe0.2Co0.2Ni0.2O3 High-Entropy Solid Solutions. Nanomaterials, 2022, 12, 36.	1.9	15
182	Correlation of the Fe content and entropy state in multiple substituted hexagonal ferrites with magnetoplumbite structure. Ceramics International, 2021, 47, 17684-17692.	2.3	14
183	A novel ceramic matrix composite based on YNbO4–TiO2 for microwave applications. Ceramics International, 2021, 47, 15424-15432.	2.3	14
184	Mechanisms of elastoplastic deformation and their effect on hardness of nanogranular Ni-Fe coatings. International Journal of Mechanical Sciences, 2022, 215, 106952.	3.6	14
185	The Interrelation of Synthesis Conditions and Wettability Properties of the Porous Anodic Alumina Membranes. Nanomaterials, 2022, 12, 2382.	1.9	14
186	Magnetotransport properties and phase separation in iron substituted lanthanum-calcium manganite. Materials Research Express, 2018, 5, 086108.	0.8	13
187	Preparation of Al3+-Co2+ co-substituted M-type SrCaNd hexaferrites and their controlled magnetic properties. AlP Advances, 2018, 8, .	0.6	13
188	Electronic structure and density of states in hexagonal BaMnO3. Modern Physics Letters B, 2018, 32, 1850186.	1.0	13
189	Morphological, structural, and magnetic characterizations of hard-soft ferrite nanocomposites synthesized via pulsed laser ablation in liquid. Materials Science and Engineering B: Solid-State Materials for Advanced Technology, 2021, 273, 115446.	1.7	13
190	Evolution of crystal structure of Ba and Ti co-doped BiFeO3 ceramics at the morphotropic phase boundary. Journal of Alloys and Compounds, 2019, 803, 1136-1140.	2.8	12
191	Soft Magnetic Amorphous Microwires for Stress and Temperature Sensory Applications. Sensors, 2019, 19, 5089.	2.1	12
192	Structural, spectral, magnetic, and electrical properties of Gd–Co-co-substituted M-type Ca–Sr hexaferrites synthesized by the ceramic method. Applied Physics A: Materials Science and Processing, 2019, 125, 1.	1.1	12
193	Alterations in the magnetic and electrodynamic properties of hard-soft Sr0.5Ba0.5Eu0.01Fe12O19/NixCuyZnwFe2O4 nanocomposites. Journal of Materials Research and Technology, 2021, 15, 1416-1429.	2.6	12
194	Properties of Mg(Fe0.8Ga0.2)2O4 + δ ceramics and films. Inorganic Materials, 2011, 47, 204-207.	0.2	11
195	Growth and structure of Mg(Fe0.8Ga0.2)2O4 â^ Î^ films. Inorganic Materials, 2011, 47, 1025-1028.	0.2	11
196	Morphology and Microstructure Evolution of Gold Nanostructures in the Limited Volume Porous Matrices. Sensors, 2020, 20, 4397.	2.1	11
197	Efficiency of Magnetostatic Protection Using Nanostructured Permalloy Shielding Coatings Depending on Their Microstructure. Nanomaterials, 2021, 11, 634.	1.9	10
198	Eco-Friendly NiO/Polydopamine Nanocomposite for Efficient Removal of Dyes from Wastewater. Nanomaterials, 2022, 12, 1103.	1.9	10

#	Article	IF	CITATIONS
199	Magnetic and Electrotransport Properties of the Anion-Deficient Manganites with Perovskite Structure. Journal of Low Temperature Physics, 2005, 139, 461-478.	0.6	9
200	Effect of high pressure on the crystal and magnetic structure and on the raman spectra in Pr0.7Ba0.3MnO3 manganite. JETP Letters, 2011, 94, 579-584.	0.4	9
201	Crystal structure and magnetic properties of nanosized Mg(Fe0.8Ga0.2)2O4-δfilms on Si substrates. Crystallography Reports, 2013, 58, 498-504.	0.1	9
202	Magnetic Ordering in BaFe \$\$_{11.9}\$\$ 11.9 In \$\$_{0.1}\$\$ 0.1 O \$\$_{19}\$\$ 19 Hexaferrite. Journal of Low Temperature Physics, 2017, 186, 44-62.	0.6	9
203	Effect of Fe doping on structure and magnetotransport properties of perovskite manganite. European Physical Journal Plus, 2018, 133, 1.	1.2	9
204	Infrared Spectroscopy, X-ray Diffraction and Neutron Diffraction Study of BaFe12â^'xAlxO19 Solid Solutions. Journal of the Korean Physical Society, 2019, 74, 584-588.	0.3	9
205	Synthesis, structure and properties of barium and barium lead hexaferrite. Journal of Magnetism and Magnetic Materials, 2019, 470, 101-104.	1.0	9
206	Phase transformations and changes in the dielectric properties of nanostructured perovskite-like LBZ composites as a result of thermal annealing. Ceramics International, 2020, 46, 14460-14468.	2.3	9
207	A study on the conductivity, dielectric, and microwave properties of SrNbxYxFe12-2xO19 (0.00 ≤ ≤Tj ET	Qq110.7	843J4 rgBT /(
208	Effect of concentration substitution on the size factor in Li1 â^ x Na x NbO3 solid solutions. Journal of Surface Investigation, 2014, 8, 1198-1200.	0.1	8
209	Structural phase transition in BaTiO3 at a constant volume under conditions of thermobaric effects. Journal of Surface Investigation, 2017, 11, 223-225.	0.1	8
210	Microwave properties of the Ga-substituted BaFe12O19hexaferrites. Materials Research Express, 2017, 4, 076106.	0.8	8
211	Refinement of the Atomic and Magnetic Structures of Solid Solutions BaFe12 – xInxO19 (x = 0.1–1.2) by the Neutron Diffraction Method. Journal of Surface Investigation, 2019, 13, 69-81.	0.1	8
212	MCC: Specific of preparation, correlation of the phase composition and electrodynamic properties. Journal of Magnetism and Magnetic Materials, 2021, 526, 167694.	1.0	8
213	Anisotropy of the electrical properties of a single crystal of BaFe11.25Ti0.75O19 M-type barium hexaferrite. Journal of Solid State Chemistry, 2021, 298, 122104.	1.4	8
214	Synthesis, Magnetic and Electrical Characteristics of Baâ€&r Hexaferrites Substituted with Samarium, Chromium and Aluminum. ChemistrySelect, 2021, 6, 470-479.	0.7	8
215	One-pot synthesis of hard/soft SrFe10O19/x(Ni0.8Zn0.2Fe1.8Cr0.2O4) nanocomposites: Electrical features and reflection losses. Ceramics International, 2022, 48, 25390-25401.	2.3	8
216	Subsolidus phase relations of Mg-Ga-Fe-O spinel solid solutions. Inorganic Materials, 2010, 46, 1019-1024.	0.2	7

#	Article	IF	CITATIONS
217	Structural and magnetic anisotropy of directionally-crystallized ferromagnetic microwires. EPJ Web of Conferences, 2018, 185, 04022.	0.1	7
218	Influence of Surface Energy on Ni-Fe Thin Films Formation Process. Materials Science Forum, 0, 946, 228-234.	0.3	7
219	Features of the Cation Distribution and Magnetic Properties of BaFe12Ââ ^{^,} ÂxYxO19 Hexaferrites. Physics of the Solid State, 2021, 63, 253-260.	0.2	7
220	Impact of Al3+ ions on magnetic and microwave properties of BaM:Ti hexaferrites. Journal of Materials Research and Technology, 2021, 11, 2235-2245.	2.6	7
221	The features of the magnetoresistance of carbon nanotubes modified with Fe. Ceramics International, 2022, 48, 19789-19797.	2.3	7
222	Neutron powder diffraction study of the anion-deficient La0.70Sr0.30MnO3.00-γmanganites. Physica Status Solidi C: Current Topics in Solid State Physics, 2009, 6, 1001-1003.	0.8	6
223	Crystallization of Mg(Fe0.8Ga0.2)2O4-δ films on silicon with SiO2 and TiO2 buffer layers. Russian Journal of Inorganic Chemistry, 2014, 59, 778-782.	0.3	6
224	Mössbauer Studies and the Microwave Properties of Al3+- and In3+-Substituted Barium Hexaferrites. Physics of the Solid State, 2018, 60, 1768-1777.	0.2	6
225	Structure and magnetic properties of FeCo nanotubes obtained in pores of ion track templates. Nano Structures Nano Objects, 2021, 26, 100691.	1.9	6
226	Correlation between Composition and Magnetic Properties of SrFe ₁₂ O ₁₉ /Co Nanocomposite Synthesized by the High Energy Ball-Milling Process. Key Engineering Materials, 0, 911, 77-85.	0.4	6
227	DMS solutions Mg(Fe1-x Ga x)2O4+δ. Doklady Physical Chemistry, 2010, 430, 39-42.	0.2	5
228	Dielectric properties of composite materials containing aligned carbon nanotubes. Inorganic Materials, 2016, 52, 1198-1203.	0.2	5
229	Extraordinary synergy in the thermal and electric properties of polymer matrix reinforced with hybrid fillers. Materialwissenschaft Und Werkstofftechnik, 2016, 47, 278-287.	0.5	5
230	Synthesis of Mg(Fe0.8Ga0.2)2O4 by Gel Combustion Using Glycine and Starch. Russian Journal of Inorganic Chemistry, 2018, 63, 1257-1261.	0.3	5
231	Study of the features of the magnetic and crystal structures of the BaFe12-D¥ ALXO19 AND BaFe12-D¥ GaXO19 substituted hexagonal ferrites. Eastern-European Journal of Enterprise Technologies, 2017, 1, 10-15.	0.3	5
232	Study of Radiation Embitterment and Degradation Processes of Li2ZrO3 Ceramic under Irradiation with Swift Heavy Ions. Ceramics, 2022, 5, 13-23.	1.0	5
233	Study of the process of the formation of Mg(Fe0.8Ga0.2)2O4 â^ Î films on Si. Russian Journal of Inorganic Chemistry, 2014, 59, 183-186.	0.3	4
234	The effect of the applied potentials difference on the phase composition of Co nanowires. Journal of Magnetic Materials, 2021, 517, 167382.	1.0	4

#	Article	IF	CITATIONS
235	Crystal Structure, Magnetic Properties and Thermal Behavior of BaFe _{11.9} In _{0.1} O ₁₉ Ferrite. Physica Status Solidi (B): Basic Research, 2022, 259, .	0.7	4
236	Magnetic Properties of the La _{0.50} Ba _{0.50} MnO ₃ Nanomanganites. Solid State Phenomena, 0, 152-153, 135-138.	0.3	3
237	Influence of charge disproportionation on microwave characteristics of Zn–Nd substituted Sr-hexaferrites. Journal of Materials Science: Materials in Electronics, 2019, 30, 6776-6785.	1.1	3
238	Structural and luminescent properties of BaFe12â^'xAlxO19 compounds. Modern Physics Letters B, 2020, 34, 2050411.	1.0	3
239	Growth mechanism study of silver nanostructures in a limited volume. Materials Chemistry and Physics, 2022, 283, 126016.	2.0	3
240	Insights into Sorption–Mineralization Mechanism for Sustainable Granular Composite of MgO-CaO-Al2O3-SiO2-CO2 Based on Nanosized Adsorption Centers and Its Effect on Aqueous Cu(II) Removal. Nanomaterials, 2022, 12, 116.	1.9	3
241	Effect of the A-Site Randomness on Magnetotransport Properties of PrBaMn ₂ O ₆ Manganites. Solid State Phenomena, 2007, 128, 187-192.	0.3	2
242	Ni-Fe Alloys as Perspective Materials for Highly Efficient Magnetostatic Shielding. Solid State Phenomena, 0, 284, 375-379.	0.3	2
243	Vibrational properties of BaFe11.1Sc0.9O19 hexaferrite at high and low temperatures. Modern Physics Letters B, 2020, 34, 2050381.	1.0	2
244	Highly efficient functional composites based on Al2O3 for combined electromagnetic and mechanical protection. Ceramics International, 2020, 46, 17584-17590.	2.3	2
245	Study of crystal and magnetic structures of manganite Pr0.7Ba0.3MnO3 at high pressure. Physics of Particles and Nuclei Letters, 2011, 8, 1063-1065.	0.1	1
246	Magnetic Phase Transitions in Zn1â´`x Mn x O. Journal of the Korean Physical Society, 2014, 64, 1457-1460.	0.3	1
247	THE INVESTIGATION OF CRYSTAL AND MAGNETIC STRUCTURES OF SOLID SOLUTIONS BaFe12-xDxO19 (D= In)	[j ETQq1 1 0.1	. 0.784314 rg
248	The Influence of Diamagnetic lons to Features of Crystalline and Magnetic Structures of BaFe <inf>11.9</inf> M <inf>0.1</inf> O <inf>19</inf> (<tex>\$ext{M}= ext{In}\$</tex> and Sc). , 2018, , .		0
249	Ni-Fe Alloys as Perspective Materials for Highly Efficient Magnetostatic Shielding. Materials Science Forum, 0, 946, 205-209.	0.3	0
250	Experimental investigation on thermodynamic properties and crystal structure of La 0.78Ba0.22MnO3 compounds. International Journal of Modern Physics B, 2020, 34, 2050101.	1.0	0
251	10.1007/s11454-008-1009-2. , 2010, 53, 49.		0
252	Influence of electrodeposition parameters on structure and micromechanical properties of thin Ni–Fe films. Proceedings of the National Academy of Sciences of Belarus Physical-Technical Series, 2020, 65, 135-144.	0.1	0